

PDF hosted at the Radboud Repository of the Radboud University Nijmegen

The version of the following full text has not yet been defined or was untraceable and may differ from the publisher's version.

For additional information about this publication click this link.

<http://hdl.handle.net/2066/34736>

Please be advised that this information was generated on 2017-12-06 and may be subject to change.

Graphene: carbon in two dimensions

Mikhail I. Katsnelson¹

¹*Institute for Molecules and Materials,*

Radboud University Nijmegen, 6525 ED Nijmegen, The Netherlands

Abstract

Carbon is one of the most intriguing elements in the Periodic Table. It forms many allotropes, some being known from ancient times (diamond and graphite) and some discovered ten to twenty years ago (fullerenes, nanotubes). Quite interestingly, the two-dimensional form (graphene) has been obtained only very recently, and immediately attracted great deal of attention. Electrons in graphene, obeying linear dispersion relation, behave like massless relativistic particles, which results in a number of very peculiar electronic properties observed in this first two-dimensional material: from an anomalous quantum Hall effect to the absence of localization. It also provides a bridge between condensed matter physics and quantum electrodynamics and opens new perspectives for carbon-based electronics.

I. TWO-DIMENSIONAL FORM OF CARBON

Carbon plays a unique role in nature. Actually, the formation of carbon in stars as a result of merging of three α -particles is a crucial process providing existence of relatively heavy chemical elements in the Universe¹. The capability of carbon atoms to form complicated networks² is a fundamental fact of organic chemistry and the base for existence of life, at least, in its known forms. Even elemental carbon demonstrates unusually complicated behavior forming a number of very different structures. Apart from diamond and graphite known from ancient times recently discovered fullerenes^{3,4,5} and nanotubes⁶ are in the focus of attention of physicists and chemists now. Thus, only three-dimensional (diamond, graphite), one-dimensional (nanotubes), and zero-dimensional (fullerenes) allotropes of carbon have been known till recently. The *two-dimensional* form was conspicuously missing, resisting any attempt of its experimental observation.

This elusive two-dimensional form of carbon has been named graphene, and, ironically, is probably the best theoretically studied carbon allotrope. Graphene - planar, hexagonal arrangements of carbon atoms is the starting point in all calculations on graphite, carbon nanotubes and fullerenes. At the same time, numerous attempts to synthesize these two-dimensional atomic crystals usually fail, ending up with nanometer-size crystallites⁷. Actually, these difficulties were not surprising, in light of a common believe that truly two-dimensional crystals (in contrast with numerous *quasi*-two-dimensional systems known before) cannot exist^{8,9,10,11,12}. Moreover, during a synthesis, any graphene nucleation sites will have very large perimeter-to-surface ratio, thus promoting collapse into other carbon allotropes.

A. Discovery of graphene

But in 2004 a group of physicists from Manchester University, led by Andre Geim and Kostya Novoselov, used a very different and, at the first glance, even naive approach to make a revolution in the field. They started with three-dimensional graphite and extracted a single sheet (a monolayer of atoms) from it by a technique called micromechanical cleavage^{13,14}, see Fig. 1. Graphite is a layered material and can be viewed as consisting of a number of two-dimensional graphene crystals weakly coupled together - exactly the property used

by the Manchester team. Moreover, by using this top-down approach and starting with large three-dimensional crystals, the researchers from Manchester avoided all the issues with the stability of small crystallites. Furthermore, the same technique has been used by the same group to obtain two-dimensional crystals of other materials¹³, such as boron-nitride, some dichalcogenides and high-temperature superconductor Bi-Sr-Ca-Cu-O. This astonishing finding sends an important message: two-dimensional crystals do exist and they are stable at ambient conditions.

Amazingly, this humble approach allows easy production of high quality, large (up to 100 μm in size) graphene crystallites, which immediately triggered enormous experimental activity^{15,16}. Moreover, the quality of the samples produced are so good, that ballistic transport¹⁴ and Quantum Hall Effect (QHE) can be easily observed^{15,16}. The former makes this new material a promising candidate for future electronic applications (ballistic field effect transistor (FET)). However, as the approach described definitely suits all the research needs, other techniques, which would allow high yield of graphene, are required for any industrial production. Among promising candidates for this role one should mention exfoliation of intercalated graphitic compounds^{17,18,19,20,21} and silicon sublimation from silicon-carbide substrates demonstrated recently by Walt de Heer's group from Georgia Institute of Technology²².

II. STABILITY ISSUES IN TWO-DIMENSIONS

The fact that two-dimensional atomic crystals do exist, and moreover, are stable under ambient conditions¹³ is amazing by itself. According to the so called Mermin-Wagner theorem¹², there should be no long-range order in two-dimensions, thus dislocations should appear in 2D crystals at any finite temperature.

A standard description²³ of atomic motion in solids assumes that amplitudes of atomic vibration \bar{u} near their equilibrium position are much smaller than interatomic distances d ; otherwise, the crystal would melt according to an empirical Lindemann criterion (at the melting point, $\bar{u} \simeq 0.1d$). Due to this smallness, thermodynamics of solids can be successfully described in a picture of an ideal gas of phonons, that is, quanta of atomic displacement waves (harmonic approximation). In three-dimensional systems this view is self-consistent in a sense that, indeed, fluctuations of atomic positions calculated in the

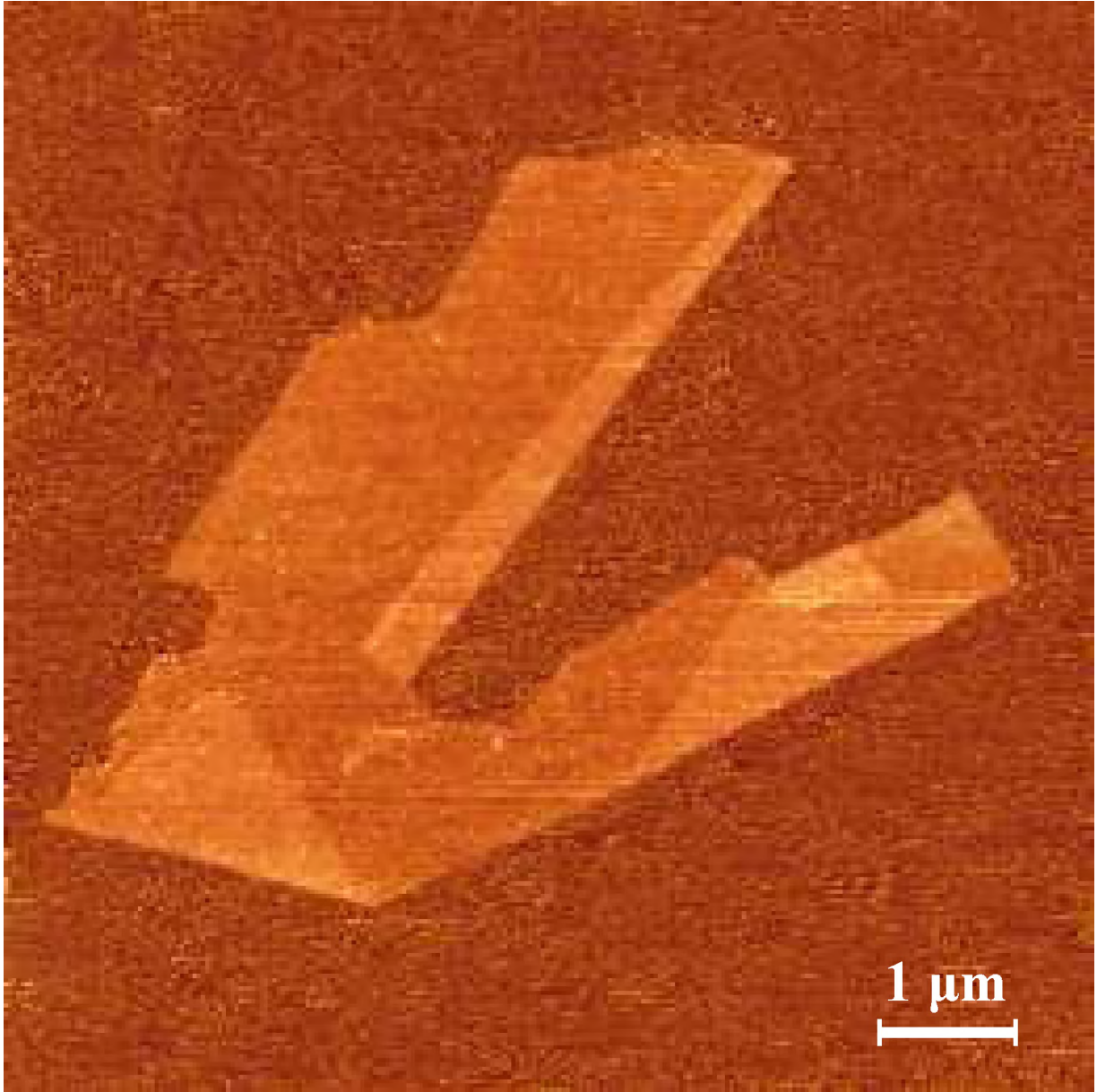


FIG. 1: Atomic force microscopy image of a graphene crystal on top of oxidized silicon substrate. Folding of the flake can be seen. The thickness of graphene measured corresponds to interlayer distance in graphite.

harmonic approximation turn out to be small, at least, for low enough temperatures. In contrast, in a two-dimensional crystal the number of long-wavelength phonons diverge at low temperatures and, thus, amplitudes of interatomic displacements calculated in the harmonic approximation are diverging^{8,9,10}). According to similar arguments, a flexible membrane

embedded into the three-dimensional space should be crumpled due to dangerous long-wavelength bending fluctuations²⁴.

However, it was demonstrated by efforts of theoreticians working on soft-condensed matter during last twenty years^{24,25,26} that these dangerous fluctuations can be suppressed by anharmonic (nonlinear) coupling between bending and stretching modes; as a result, the single-crystalline membrane can exist but should be “rippled”. This means arising of “roughness fluctuations” with a typical height scaled with the sample size L as L^ζ , with $\zeta \simeq 0.6$. Indeed, the ripples are observed in graphene and play an important role in their electronic properties²⁷. However, these investigations have just started (one can mention a few recent works on Raman spectroscopy on graphene^{28,29}), and “phononic” aspects of two-dimensionality in graphene are still very poorly understood.

Another important issue is a role of defects in thermodynamic stability of two-dimensional crystals. Finite concentration of such defects as dislocations and disclinations would destroy long-range translational and orientational order, respectively. The detailed analysis²⁴ shows that the dislocations in *flexible* membranes have a finite energy (of order of cohesion energy E_{coh}), due to screening of bending deformations, whereas the energy of disclinations is logarithmically divergent with the size of crystallite. This means that, rigorously speaking, the translational long-range order (but not the orientational one) is broken at any finite temperatures T . However, the density of dislocations in the equilibrium is exponentially small for large enough E_{coh} (in comparison with the thermal energy $k_B T$) so, in practice, this restriction is not very serious for strongly bonded two-dimensional crystals like graphene.

III. ELECTRONIC STRUCTURE OF GRAPHENE: LINEAR DISPERSION RELATION

The electronic structure of graphene follows already from simple nearest-neighbor tight-binding approximation³⁰. Graphene has two atoms per unit cell, which results in two “conical” points per Brillouin zone with the band crossing, K and K' . Near these crossing points the electron energy is linearly dependent on the wave vector. Actually, this behavior follows from symmetry considerations³¹ and, thus, is robust with respect to long-range hopping processes (Figure 2).

What makes graphene so attractive for research, is that the spectrum closely resembles

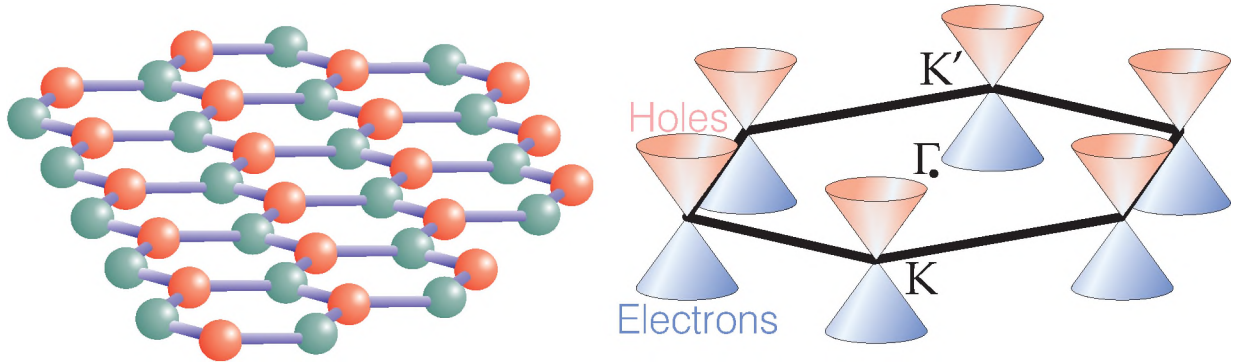


FIG. 2: Left: Crystallographic structure of graphene. Atoms from different sublattices (A and B) are marked by different colors. Right: Band structure of graphene in the vicinity of the Fermi level. Conduction band touches valence band at K and K' points.

the Dirac spectrum for massless fermions^{32,33}. The Dirac equation describes relativistic quantum particles with spin $1/2$, such as electrons. The essential feature of the Dirac spectrum following from the basic principles of quantum mechanics and relativity theory is the existence of antiparticles. More specifically, states at positive and negative energies (electrons and positrons) are intimately linked (conjugated), being described by different components of the same spinor wavefunction. This fundamental property of the Dirac equation is often referred to as the charge-conjugation symmetry. For Dirac particles with mass m there is a gap between minimal electron energy, $E_0 = mc^2$, and maximal positron energy, $-E_0$ (c is the speed of light). When the electron energy $E \gg E_0$ the energy is linearly dependent on the wavevector \mathbf{k} , $E = \hbar ck$. For *massless* Dirac fermions, the gap is zero and this linear dispersion law holds at any energies. For this case, there is an intimate relation between the spin and motion of the particle: spin can be only directed along the propagation direction (say, for particles) or only opposite to it (for antiparticles). In contrast, massive spin- $1/2$ particles can have *two* values of spin projection on any axis. In a sense we have a unique situation here: charged massless particles. Although it is a popular textbook example - no such particles have been observed before.

The fact that charge carriers in graphene are described by the Dirac-like spectrum, rather than the usual Schrödinger equation for nonrelativistic quantum particles, can be seen as a consequence of graphene's crystal structure, which consists of two equivalent carbon sublattices A and B (see the Figure 2). Quantum mechanical hopping between the sublattices

leads to the formation of two energy bands, and their intersection near the edges of the Brillouin zone yields the conical energy spectrum. As a result, quasiparticles in graphene exhibit a linear dispersion relation $E = \hbar k v_F$, as if they were massless relativistic particles (for example, photons) but the role of the speed of light is played here by the Fermi velocity $v_F \approx c/300$. Due to the linear spectrum, one can expect that graphene's quasiparticles behave differently from those in conventional metals and semiconductors where the energy spectrum can be approximated by a parabolic (free-electron-like) dispersion relation.

IV. CHIRAL DIRAC ELECTRONS

Although the linear spectrum is important, it is not its only essential feature. Above zero energy, the current carrying states in graphene are, as usual, electron-like and negatively charged. At negative energies, if the valence band is not full, its unoccupied electronic states behave as positively charged quasiparticles (holes), which are often viewed as a condensed-matter equivalent of positrons. Note however that electrons and holes in condensed matter physics are normally described by separate Schrödinger equations, which are not in any way connected (as a consequence of the so called Seitz sum rule³⁴, the equations should also involve different effective masses). In contrast, electron and hole states in graphene should be interconnected, exhibiting properties analogous to the charge-conjugation symmetry in the quantum electrodynamics (QED)^{31,32,33}. For the case of graphene, the latter symmetry is a consequence of its crystal symmetry because graphene's quasiparticles have to be described by two-component wavefunctions, which is needed to define relative contributions of sublattices A and B in quasiparticles' make-up. The two-component description for graphene is very similar to the one by spinor wavefunctions in QED but the "spin" index for graphene indicates sublattices rather than the real spin of electrons and is usually referred to as pseudospin σ . This allows one to introduce chirality³³, that is formally a projection of pseudospin on the direction of motion, which is positive and negative for electrons and holes, respectively.

The description of electron spectrum of graphene in terms of Dirac massless fermions is a kind of continuum-medium description applicable for electron wavelengths much larger than interatomic distance. However, even at these space scales there is still a reminiscence of the structure of elementary cell, that is, existence of two sublattices. In terms of the continuum

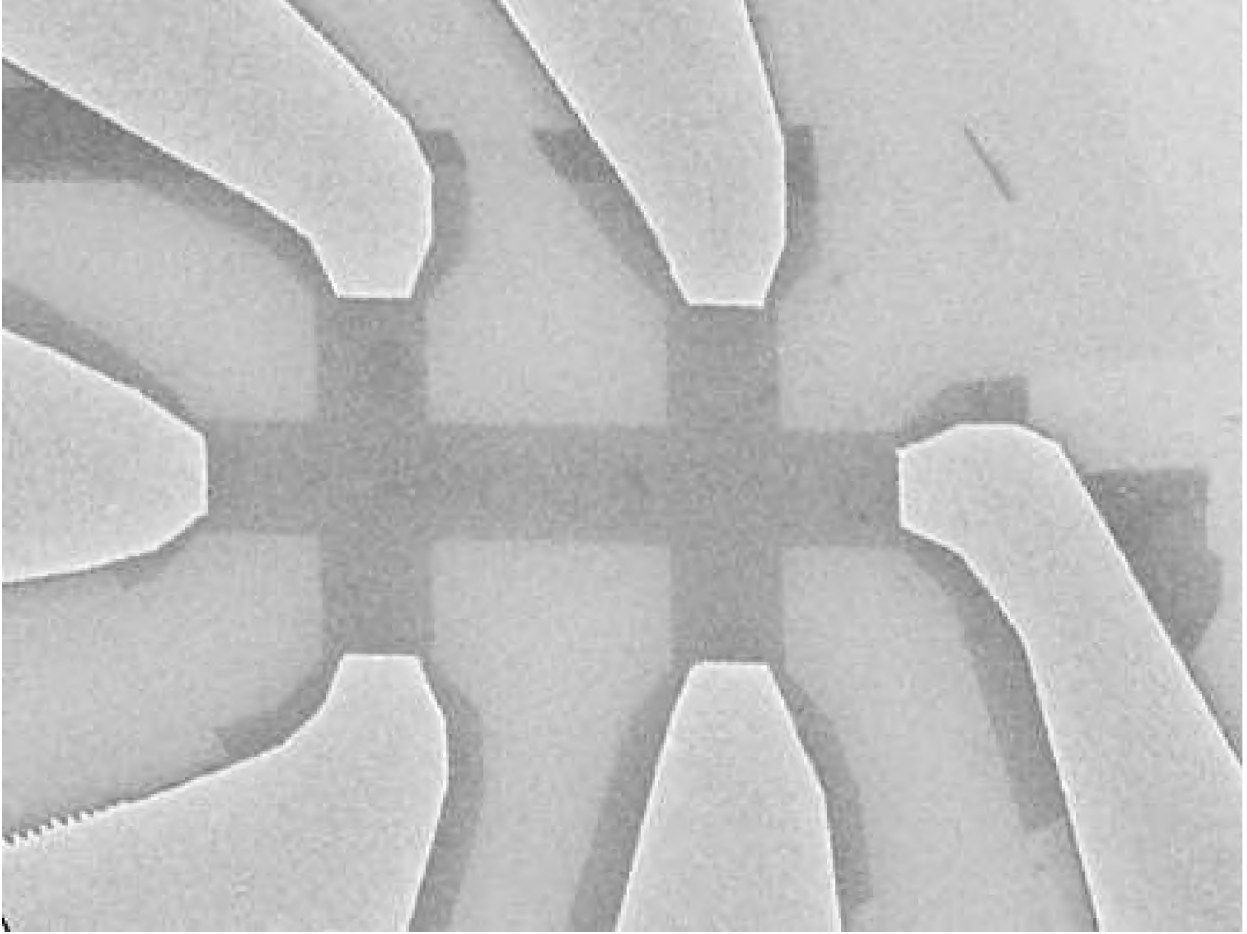


FIG. 3: SEM micrograph of a graphene device. Graphene crystal has been connected by golden electrodes and patterned into Hall bar geometry by e-beam lithography with subsequent reactive plasma etching. The width of the channel is $1\mu m$. (Courtesy of K. Novoselov and A. Geim)

field theory, this can be described only as *internal* degree of freedom of charge carriers which is just the chirality.

This description is based on oversimplified nearest-neighbor tight-binding model. However, it was proven experimentally that charge carriers in graphene do have this Dirac-like gapless energy spectrum^{15,16}. This was demonstrated in transport experiments (Fig. 3) via investigation of Schubnikov - de Haas effect, that is, oscillations of resistivity in high magnetic fields at low temperatures.

V. ANOMALOUS QUANTUM HALL EFFECT IN GRAPHENE

Magnetooscillation effects such as de Haas - van Alphen (oscillations of the magnetization) or Schubnikov - de Haas effect (magneto-oscillations in the resistance) are among the most straightforward and reliable tools to investigate electron energy spectrum in metals and semiconductors³⁵. In two-dimensional systems with a constant magnetic field \mathbf{B} perpendicular to the system plane the energy spectrum is discrete (Landau quantization). For the case of massless Dirac fermions the energy spectrum takes the form (see, e.g.,³⁶)

$$E_{\nu\sigma} = \pm \sqrt{2 |e| B \hbar v_F^2 (\nu + 1/2 \pm 1/2)} \quad (1)$$

where v_F is the electron velocity, $\nu = 0, 1, 2, \dots$ is the quantum number and the term with $\pm 1/2$ is connected with the chirality (Figure 4). Just to remind that in the usual case of parabolic dispersion relation the Landau level sequence is $E = \hbar\omega_c(\nu + 1/2)$ where ω_c is the frequency of electron rotation in the magnetic field (cyclotron frequency)³⁵.

By changing the value of magnetic field at a given electron concentration (or, vice versa, electron concentration for a given magnetic field) one can tune the Fermi energy E_F with one of the Landau levels. Such crossing changes drastically all properties of metals (or semiconductors) and, thus, different physical quantities will oscillate with the value of the inverse magnetic field. By measuring the period of these oscillations $\Delta(1/B)$ we obtain an information about the area \mathcal{A} inside the Fermi surface (for two-dimensional systems, this area is just proportional to the charge-carrier concentration n). The amplitude of the oscillations allows us to measure the effective cyclotron mass which is proportional to $\partial\mathcal{A}/\partial E_F$ ^{34,35}. For the case of massless Dirac fermions (linear dependence of the electron energy on its momentum) this quantity should be proportional to \sqrt{n} which was exactly the behavior observed simultaneously by the Manchester group and a group of Philip Kim and Horst Stormer from Columbia University^{15,16} (see Figure 5).

An important peculiarity of the Landau levels for massless Dirac fermions is the existence of zero-energy states (with $\nu = 0$ and minus sign in equation (1)). This situation differs essentially from usual semiconductors with parabolic bands where the first Landau level is shifted by $1/2 \hbar\omega_c$. As it has been shown by the Manchester and the Columbia groups^{15,16}, the existence of the zero-energy Landau level leads to an anomalous quantum Hall effect (QHE) with *half-integer* quantization of the Hall conductivity (Fig. 6, upper panel), instead of *integer* one (for a review of the QHE, see, e.g., Ref.³⁷). Usually, all Landau levels have the

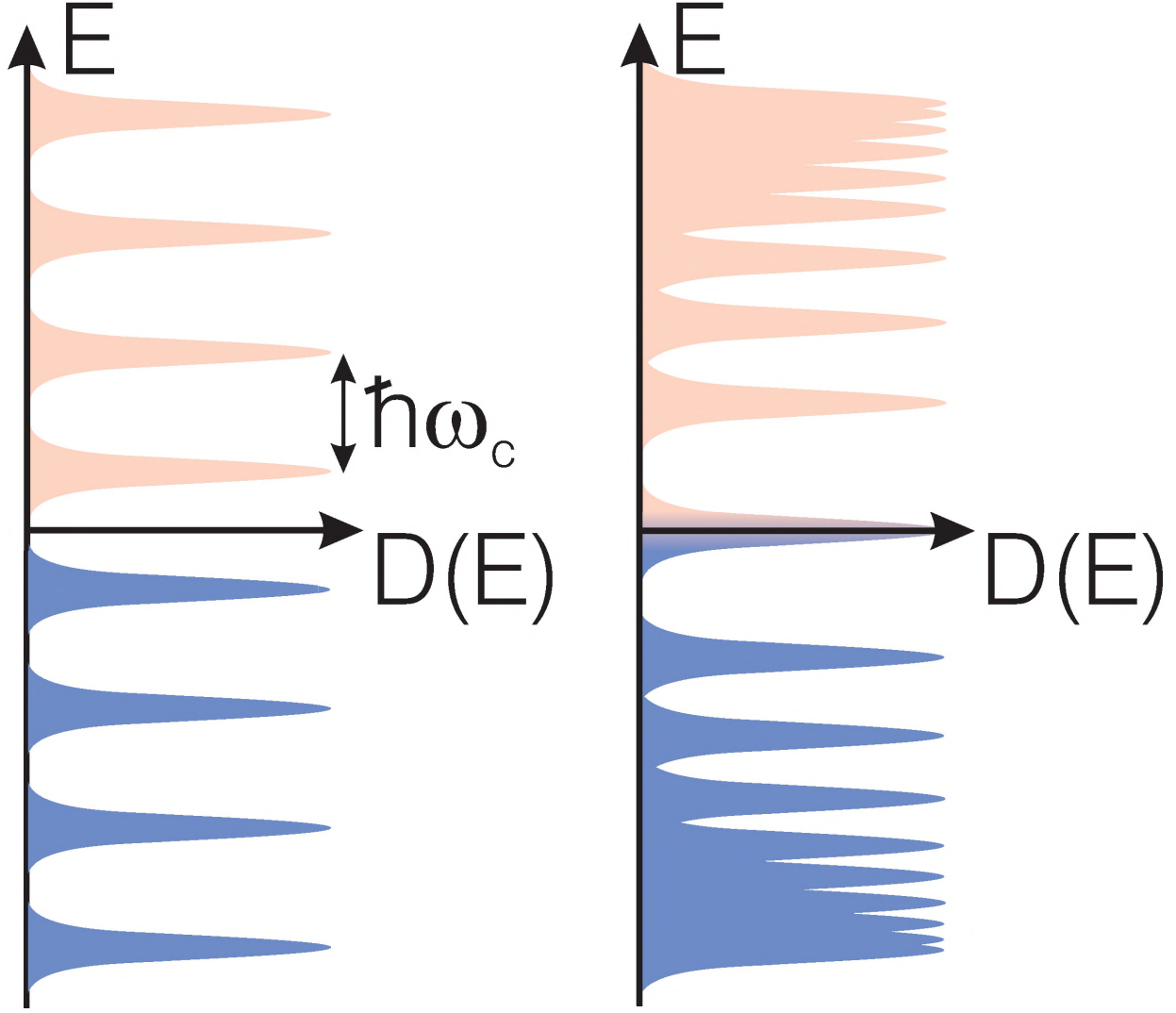


FIG. 4: Landau levels for Schrödinger electrons with two parabolic bands touching each other at zero energy (left panel). Landau levels for Dirac electrons (right panel).

same degeneracy (a number of electron states with a given energy) which is just proportional to the magnetic flux through the system. As a result, the plateaus in the Hall conductivity corresponding to the filling of first ν levels are just integer (in units of the conductance quant e^2/h). For the case of massless Dirac electrons, the zero-energy Landau level has twice smaller degeneracy than any other level (it corresponds to the minus sign in the equation (1) whereas p -th level with $p \geq 1$ are obtained twice, with $\nu = p$ and minus sign, and with $\nu = p - 1$ and plus sign). A discovery of this anomalous QHE was the most direct evidence of the Dirac fermions in graphene^{15,16}.

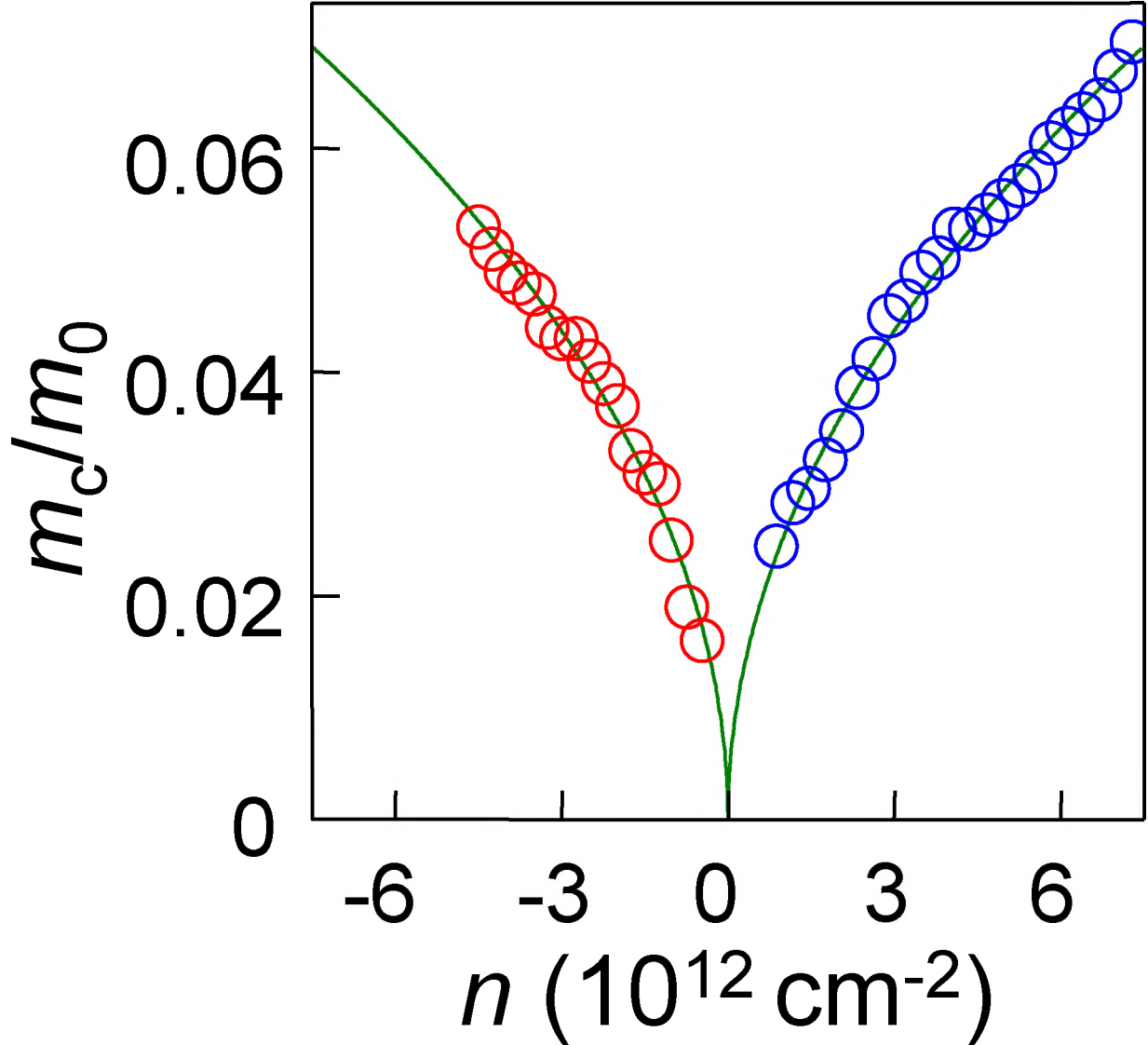


FIG. 5: Electrons and holes cyclotron mass as a function of carrier concentration in graphene. The square-root dependence suggests linear dispersion relation.

A. Index theorem

The deepest view on the origin of zero-energy Landau level and thus anomalous QHE is provided by a famous Atiyah-Singer index theorem which plays an important role in modern quantum field theory and theory of superstrings³⁸. The Dirac equation has a charge-conjugation symmetry between electrons and holes. This means that for any electron state with a positive energy E a corresponding conjugated hole state with the energy $-E$ should

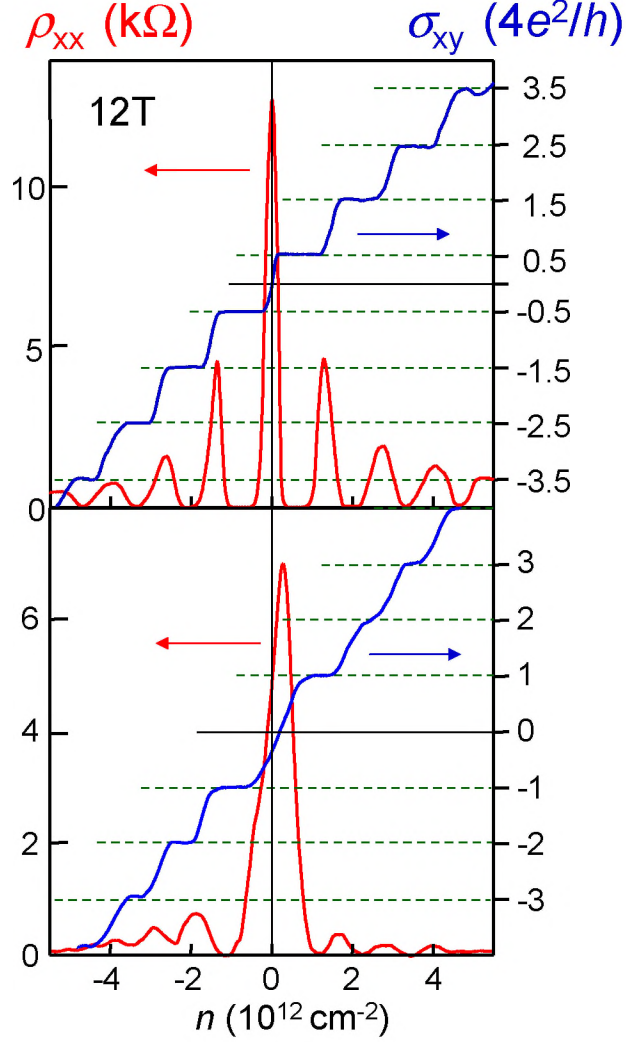


FIG. 6: Resistivity (red curves) and Hall conductivity (blue curves) as a function of carrier concentration in graphene (upper panel) and bi-layer graphene (lower panel).

exist. However, the states with zero energy can be, in general, anomalous. For curved space (e.g., for a deformed graphene sheet with some defects of crystal structure) and/or in the presence of so called “gauge fields” (usual electromagnetic field provides just a simplest example of these fields) sometimes an existence of states with zero energy is guaranteed by topological reasons, this states being chiral (in our case this means that depending on the sign of the magnetic field there is only sublattice A or sublattice B states which contribute to the zero-energy Landau level). This means, in particular, that the number of these states expressed in terms of total magnetic flux is a topological invariant and remains the same even if the magnetic field is inhomogeneous¹⁵. This is an important conclusion since the ripples

on graphene create effective inhomogeneous magnetic fields of magnitude up to 1T leading, in particular, to suppression of the weak localization²⁷. However, due to these topological arguments they cannot destroy the anomalous QHE in graphene. For further insight in to the applications of the index theorem to two-dimensional systems, and, in particular, to graphene see Refs.^{39,40}.

B. Quasi-classical consideration: Berry phase.

An alternative view on the origin of the anomalous QHE in graphene is based on the concept of “Berry phase”⁴¹. Since the electron wave function is a two-component spinor, it has to change sign when the electron moves along the close contour. Thus the wave function gains an additional phase $\phi = \pi$. In quasiclassical terms (see, e.g., Refs.^{34,42}), stationary states are nothing but electron standing waves and they can exist if the electron orbit contains, at least, half of the wavelength. Due to additional phase shift by the Berry phase, this condition is satisfied already for the zeroth length of the orbit, that is, for zero energy!

Other aspects of the QHE in graphene are considered in papers^{43,44,45,46}.

VI. ANOMALOUS QUANTUM HALL EFFECT IN BILAYER GRAPHENE

In relativistic quantum mechanics, chirality is intimately connected with relativistic considerations which dictates, at the same time, linear energy spectrum for massless particles. Discovery of graphene opens a completely new opportunity, to investigate *chiral* particles with *parabolic (non-relativistic)* energy spectrum! This is the case of *bilayer* graphene⁴⁷. For two carbon layers, the nearest-neighbor tight-binding approximation predicts a gapless state with *parabolic* touching in K and K' points, instead of conical one^{47,48}. More accurate consideration⁴⁹ gives a very small band overlap (about 1.6 meV) but at larger energies the bilayer graphene can be treated as the gapless semiconductor. At the same time, the electron states are still characterized by chirality and by the Berry phase (which is equal, in this case, 2π instead of π). Exact solution of the quantum mechanical equation for this kind of spectrum in a presence of homogeneous magnetic field gives the result^{47,48} $E_\nu \propto \sqrt{\nu(\nu - 1)}$ and, thus, the number of states with zero energy is twice larger than for the case of monolayer

($\nu = 0$ and $\nu = 1$). As a result, the QHE for bilayer graphene differs from both single-layer one and conventional semiconductors, as it was found experimentally⁴⁷ by the Manchester team (Fig. 6, lower panel).

VII. TUNNELING OF CHIRAL PARTICLES

Chiral nature of electron states in the bilayer (as well as for the case of single-layer graphene) is of crucial importance for electron tunnelling through potential barriers and, thus, physics of electronic devices such as “carbon transistors”⁵⁰.

A. Quantum tunneling

Quantum tunneling is a consequence of very general laws of quantum mechanics, such as the famous Heisenberg uncertainty relations. A classical particle cannot propagate through a region where its potential energy is higher than its total energy (figure 7). However, due to the uncertainty principle, for the case of quantum particle it is impossible to know exact values of its coordinate and velocity, and, thus, its kinetic and potential energy at the same time instant. Therefore, penetration through the “classically forbidden” region turns out to be possible. This phenomenon is widely used in modern electronics starting from pioneering works by L. Esaki⁵¹.

B. Klein paradox in graphene

When potential barrier is smaller than a gap separating electron and hole bands in semiconductors, the penetration probability decays exponentially with the barrier height and width. Otherwise, a resonant tunneling possible when the energy of propagating electron coincides with one of the hole energy levels inside the barrier. Surprisingly, in the case of graphene the transmission probability for normally incident electrons is always equal to unity, irrespective to the height and width of the barrier^{50,52,53}. In terms of quantum electrodynamics, this behavior is related to the phenomenon known as the Klein paradox^{50,54,55,56}. This term usually refers to a counter intuitive relativistic process in which an incoming electron starts penetrating through a potential barrier if its height exceeds twice the electron’s

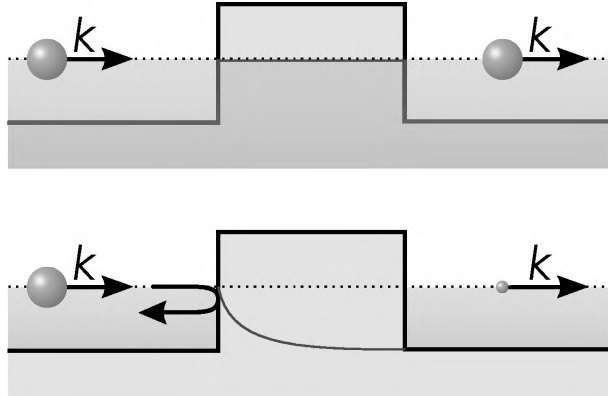


FIG. 7: Tunneling in graphene (top panel) and in conventional semiconductor (lower panel). The amplitude of electron wavefunction (red line) remains constant in case of graphene and drops exponentially for conventional tunneling. The size of the ball indicate the amplitude of the incident and transmitted wavefunction.

rest energy mc^2 . In this case, the transmission probability T depends only weakly on the barrier height, approaching the perfect transparency for very high barriers, in stark contrast to the conventional, nonrelativistic tunnelling. This relativistic effect can be attributed to the fact that a sufficiently strong potential, being repulsive for electrons, is attractive for positrons and results in positron states inside the barrier, which align in energy with the electron continuum outside. Matching between electron and positron wavefunctions across the barrier leads to the high-probability tunnelling described by the Klein paradox. In other words, it reflects an essential difference between nonrelativistic and relativistic quantum mechanics. In the former case, we can measure accurately either position of the electron or its velocity but not both of them simultaneously. In the relativistic quantum mechanics, we cannot measure even electron position with arbitrary accuracy since when we try to do this we create electron-positron pairs from the vacuum and we cannot distinguish our original electron from these newly created electrons. Graphene opens a way to investigate this counterintuitive behavior in a relatively simple bench-top experiment, whereas originally it was connected with only some very exotic phenomena such as collisions of ultraheavy nuclei or black hole evaporations (for more references and explanations, see^{50,56}).

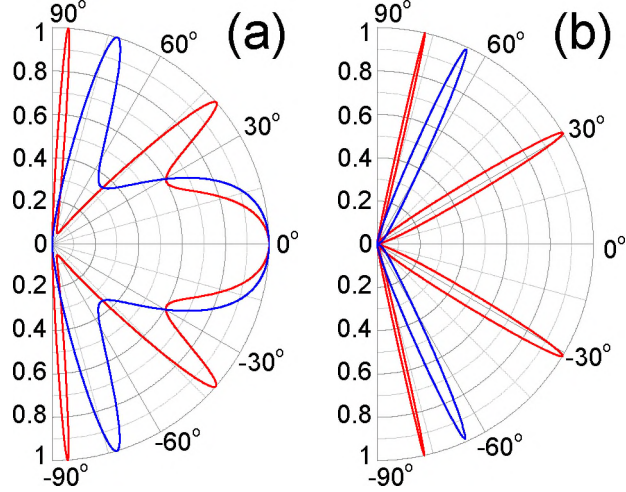


FIG. 8: Transmission probability T through a 100-nm-wide barrier as a function of the incident angle for single- (a) and bi-layer (b) graphene. The electron concentration n outside the barrier is chosen as $0.5 \times 10^{12} \text{ cm}^{-2}$ for all cases. Inside the barrier, hole concentrations p are 1×10^{12} and $3 \times 10^{12} \text{ cm}^{-2}$ for red and blue curves, respectively (such concentrations are most typical in experiments with graphene). This corresponds to the Fermi energy E of incident electrons ≈ 80 and 17 meV for single- and bi-layer graphene, respectively, and $\lambda \approx 50 \text{ nm}$. The barrier heights are (a) 200 and (b) 50 meV (red curves) and (a) 285 and (b) 100 meV (blue curves).

C. Tunneling of chiral quasiparticles in bilayer graphene

From the point of view of possible applications it is a rather bad news since it means that the “carbon transistor” from the single-layer graphene cannot be closed by any external gate voltage. On the contrary, it was shown in Ref.⁵⁰ that the chiral tunnelling for the case of *bilayer* leads to even stronger suppression of the normally incident electron penetration (Figure 8) than in conventional semiconductors. It means that by creating a potential barrier (with external gate) one can manipulate the transmission probability for ballistic electrons in bilayer graphene. At the same time, there is always some “magic angle” where the penetration probability equals unity (Figure 8), which should be also taken into account for a design of future carbon-based electronic devices.

D. Absence of localization

The discussed tunneling anomalies in single- and bilayer graphene systems are expected to play an important role in their transport properties, especially in the regime of low carrier concentrations where disorder induces significant potential barriers and the systems are likely to split into a random distribution of p-n junctions. In conventional 2D systems, strong enough disorder results in electronic states that are separated by barriers with exponentially small transparency^{57,58}. This is known to lead to the Anderson localization. In contrast, in both graphene materials all potential barriers are rather transparent at least for some angles which does not allow charge carriers to be confined by potential barriers that are smooth on atomic scale. Therefore, different electron and hole “puddles” induced by disorder are not isolated but effectively percolate, thereby suppressing localization. This consideration can be important for the understanding of the minimal conductivity $\approx e^2/h$ observed experimentally in both single-layer¹⁵ and bilayer⁴⁷ graphene. Further discussion of this minimal conductivity phenomenon in terms of quantum relativistic effects can be found in Refs.^{59,60,61}.

VIII. GRAPHENE DEVICES

The unusual electronic properties of this new material make it a promising candidate for future electronic applications. The typical mobility easily achieved at the current state of “graphene technology” is around $20.000 \text{ cm}^2/V \cdot \text{s}$, which is already an order of magnitude higher than that of modern silicon transistors, and it continues to grow as the quality of graphene samples is improved. This insures ballistic transport on sub-micron distances - the holy grail for any electronic engineer. Probably the best candidates for graphene-based field effect transistors will be devices based on quantum dots and those utilizing $p - n$ junctions in bilayer graphene^{50,62}.

Another promising direction of investigation is spin-valve devices. Due to negligible spin-orbit coupling, spin polarization in graphene survives over submicron distances, which recently has allowed observation of spin-injection and spin-valve effect in this material⁶³. It also has been shown by the group of A. Morpurgo from Delft University that superconductivity can be induced in graphene due to proximity effect⁶⁴. Moreover, the value of

supercurrent can be controlled by an external gate voltage, which can lead to the creation of superconducting FET.

Whenever the applications mentioned are a matter of further investigations, there are some areas where graphene can be used straightaway. Gas sensors are one of them. It has been shown by the Manchester group that graphene can absorb gas molecules from the surrounding atmosphere, which results in doping of the graphene layer with electrons or holes, depending on the nature of the absorbed gas⁶⁵. By monitoring changes of resistivity one can sense minute concentrations of certain gases present in the environment. Moreover, the sensitivity is so high that one can detect an individual event of a single molecule attaching to the surface of graphene gas sensor⁶⁵.

IX. CONCLUSIONS

It is impossible, in this short paper, to review all aspects of graphene physics and chemistry. We hope, however, that the examples considered above already demonstrate its great interest for both fundamental research (a new, unexpected bridge between condensed matter and quantum field theory) and possible applications. First of all, graphene is the first example of truly two-dimensional crystals, in contrast with numerous *quasi*-two-dimensional crystals known before. This opens many interesting questions concerning thermodynamics, lattice dynamics and structural properties of such systems. Further, being a gapless semiconductor with linear energy spectrum the single-layer graphene provides a realization of two-dimensional massless Dirac fermion system which is of crucial importance for understanding unusual electronic properties, such as anomalous QHE, absence of the Anderson localization, etc. The bilayer graphene has a very unusual gapless parabolic spectrum giving an example of the system with electron wave equation different from both Dirac and Schrödinger ones. These peculiarities are important for development of new electronic devices such as carbon transistors.

Acknowledgements. I am thankful to Kostya Novoselov and Andre Geim for many helpful discussions. This work was supported by the Stichting voor Fundamenteel Onderzoek der

Materie (FOM), the Netherlands.

- ¹ Fowler, W. A., *Rev. Mod. Phys.* (1984) **56**, 149.
- ² Pauling, L., *The Nature of the Chemical Bond*, Cornell Univ. Press, Ithaca, N.Y. (1960).
- ³ Curl, R. F., *Rev. Mod. Phys.* (1997) **69**, 691.
- ⁴ Kroto, H., *Rev. Mod. Phys.* (1997) **69**, 703.
- ⁵ Smalley, R. E. *Rev. Mod. Phys.* (1997) **69**, 723.
- ⁶ Iijima, S. *Nature* (1991) **354**, 56.
- ⁷ Oshima, C. and Nagashima, A., *J. Phys.: Condens. Matter* (1997) **9**, 1.
- ⁸ Peierls, R. E., *Helv. Phys. Acta* (1934) **7**, 81.
- ⁹ Peierls, R. E., *Ann. Inst. H. Poincare* (1935) **5**, 177.
- ¹⁰ Landau, L. D., *Phys. Z. Sowjet Union* (1937) **11**, 26.
- ¹¹ Landau, L. D. and Lifshitz, E. M., *Statistical Physics, Part I*, Pergamon Press, Oxford (1980).
- ¹² Mermin, N. D., *Phys. Rev.* (1968) **176**, 250.
- ¹³ Novoselov, K. S., *et. al.*, *PNAS* (2005) **102**, 10451.
- ¹⁴ Novoselov, K. S., *et. al.*, *Science* (2004) **306**, 666.
- ¹⁵ Novoselov, K. S. *et. al.*, *Nature* (2005) **438**, 197.
- ¹⁶ Zhang, Y. *et. al.*, *Nature* (2005) **438**, 201.
- ¹⁷ Dresselhaus, M. S. and Dresselhaus, G., *Adv. Phys.* (2002) **51**, 1.
- ¹⁸ Shioyama, H., *J. Mater. Sci. Lett.* (2001) **20**, 499.
- ¹⁹ Viculis, L. M., *et. al.*, *Science* (2003) **299**, 1361.
- ²⁰ Horiuchi, S., *et. al.*, *Appl. Phys. Lett.* (2004) **84**, 2403.
- ²¹ Stankovich, S. *et. al.*, *J. Mater. Chem.* (2006) **16**, 155.
- ²² Berger, C. *et al.*, *J. Phys. Chem. B* (2004) **108**, 19912.
- ²³ Born, M. and Huang, K. *Dynamical Theory of Crystal Lattices*, Oxford Univ. Press, Oxford (1998).
- ²⁴ Nelson, D. R., Piran, T., and Weinberg, S. (Editors), *Statistical Mechanics of Membranes and Surfaces*, World Scientific, Singapore (2004).
- ²⁵ Nelson, D. R. and Peliti, L. *J. Physique* (1987) **48**, 1085.
- ²⁶ Radzihovsky, L. and Le Doussal, P. *Phys. Rev. Lett.* (1992) **69**, 1209.

- ²⁷ Morozov, S. V. *et. al.*, *Phys. Rev. Lett.* (2006) **97**, 016801.
- ²⁸ Ferrari, A. C. *et. al.*, *Phys. Rev. Lett.* (2006) **97**, 187401.
- ²⁹ Graf, D. *et. al.*, *E-print at arxiv.org: cond-mat/0607562*.
- ³⁰ Wallace, P. R., *Phys. Rev.* (1947) **71**, 622.
- ³¹ Slonczewski, J. C., and Weiss, P. R., *Phys. Rev.* (1958) **109**, 272.
- ³² Semenoff, G. W., *Phys. Rev. Lett.* (1984) **53**, 2449.
- ³³ Haldane, F. D. M., *Phys. Rev. Lett.* (1988) **61**, 2015.
- ³⁴ Vonsovsky, S. V. and Katsnelson, M. I. *Quantum Solid State Physics*, Springer, N.Y. (1989).
- ³⁵ Ashcroft, N. W. and Mermin N. D. *Solid State Physics*, Holt, Rinehart and Winston, N.Y. (1976).
- ³⁶ Gusynin, V. P. and Sharapov, S. G., *Phys. Rev. B* (2005) **71**, 125124.
- ³⁷ Prange, R. E. and Girvin, S. M. (Editors), *The Quantum Hall Effect*, Springer, N.Y. (1987).
- ³⁸ Kaku, M. *Introduction to Superstrings*, Springer, N.Y. (1988).
- ³⁹ Tenjinbayashi, Y., *et. al.*, *Ann. Phys. (N.Y.)*, in press (doi:10.1016/j.aop.2006.02.013).
- ⁴⁰ Pachs, J. K. and Stone, M., *E-print at arxiv.org: E-print at arxiv.org: cond-mat/0607394*.
- ⁴¹ Shapere, A. and Wilczek, F. (Editors), *Geometrical Phases in Physics*, World Scientific, Singapore (1989).
- ⁴² Mikitik, G. P. and Sharlai, Yu. V., *Phys. Rev. Lett.* (1999) **82**, 2147.
- ⁴³ Abanin, D. A. *et. al.*, *Phys. Rev. Lett.* (2006) **96**, 176803.
- ⁴⁴ Gusynin, V. P. and Sharapov, S. G., *Phys. Rev. Lett.* (2005) **95**, 146801.
- ⁴⁵ Peres, N. M. R. *et. al.*, *Phys. Rev. B* (2006) **73**, 125411.
- ⁴⁶ Castro Neto, A. H. *et. al.*, *Phys. Rev. B* (2006) **73**, 205408.
- ⁴⁷ Novoselov, K. S. *et. al.* *Nature Phys.* (2006) **2**, 177.
- ⁴⁸ McCann, E. and Falko, V. I. *Phys. Rev. Lett.* (2006) **96**, 086805.
- ⁴⁹ Partoens, B. and Peeters, F. M. *Phys. Rev. B* (2006) **74**, 075404.
- ⁵⁰ Katsnelson, M. I. *et. al.*, *Nature Phys.* (2006) **2**, 620.
- ⁵¹ Esaki, L. *Phys. Rev.* (1958) **109**, 603.
- ⁵² Milton Pereira, J. Jr. *et. al.*, *Phys. Rev. B* (2006) **74**, 045424.
- ⁵³ Cheianov, V. V. and Falko, V. I., *Phys. Rev. B* (2006) **74**, 041403(R).
- ⁵⁴ Klein, O. *Z. Phys.* (1929) **53**, 157.
- ⁵⁵ Dombey, N., and Caloggeracos, A. *Phys. Rep.* (1999) **315**, 41.

- ⁵⁶ Calogeracos, A. *Nature Phys.* (2006) **2**, 579.
- ⁵⁷ Ziman, J. M. *Models of Disorder*, Cambridge Univ. Press, Cambridge (1979).
- ⁵⁸ Lifshitz, I. M., Gredeskul, S. A., and Pastur, L. A. *Introduction to the Theory of Disordered Systems*, Wiley, N.Y. (1988).
- ⁵⁹ Katsnelson, M. I. *Eur. Phys. J. B* (2006) **51**, 157.
- ⁶⁰ Katsnelson, M. I. *Eur. Phys. J. B* (2006) **52**, 151.
- ⁶¹ Tworzydło, J. *et al.*, *Phys. Rev. Lett.* (2006) **96**, 246802.
- ⁶² Nilsson, J., *et al.*, *E-print at arxiv.org: cond-mat/0607343*.
- ⁶³ Hill, E., *et al.*, *IEEE Transactions on Magnetics* (2006) **42**, 2694.
- ⁶⁴ Heersche, H. B., *et al.* *Conference: Nanophysics: from Fundamentals to Applications*, Vietnam, Hanoi, August 6-12, 2006.
- ⁶⁵ Schedin, F. *et al.*, *E-print at arxiv.org: cond-mat/0610809*.